See related commentary on pg 2343

Human Cutaneous Melanomas Lacking MITF and Melanocyte Differentiation Antigens Express a Functional Axl Receptor Kinase

Marialuisa Sensi[1], Mara Catani[1,5], Giancarlo Castellano[2,6], Gabriella Nicolini[1], Federica Alciato[3], Gabrina Tragni[4], Giuseppina De Santis[2], Ilaria Bersani[1], Giancarlo Avanzi[3], Antonella Tomassetti[2], Silvana Canevari[2] and Andrea Anichini[1]

Axl, a member of the TAM (Tyro3, Axl, Mer) family of receptor tyrosine kinases, displays an increasingly important role in carcinogenesis. Analysis of 58 cutaneous melanoma lines indicated that Axl was expressed in 38% of them, with significant overrepresentation in *NRAS*- compared with *BRAF*-mutated tumors. Axl activation could be induced by autocrine production of its ligand, Gas6, in a significant fraction of Axl-positive tumors. Pearson's correlation analysis on expression data from five data sets of melanoma lines identified several transcripts correlating positively or negatively with *Axl*. By functionally grouping genes, those inversely correlated were involved in melanocyte development and pigmentation, whereas those positively correlated were involved in motility, invasion, and microenvironment interactions. Accordingly, Axl-positive melanomas did not express microphthalmia transcription factor (MITF) and melanocyte differentiation antigens (MDAs) such as MART-1 and gp100 and possessed a greater *in vitro* invasive potential compared with Axl-negative ones. Motility, invasivity, and ability to heal a wound or to migrate across an endothelial barrier were inhibited *in vitro* by Axl knockdown. Pharmacological inhibition of Axl using the selective inhibitor R428 had comparable effects in reducing migration and invasion. These results suggest that targeted inhibition of Axl signaling in the subset of melanomas lacking MITF and MDAs may represent a novel therapeutic strategy.

Journal of Investigative Dermatology (2011) **131,** 2448–2457; doi:10.1038/jid.2011.218; published online 28 July 2011

INTRODUCTION

Melanoma is a skin malignancy with a complex and heterogeneous etiology. Activating mutations in *BRAF* and *NRAS* are involved in its development with an occurrence of 41 and 18%, respectively (Lee *et al.*, 2011). High-throughput genomic screens have recently discovered numerous alterations occurring at lower frequency (Curtin *et al.*, 2006; Palavalli *et al.*, 2009; Prickett *et al.*, 2009; Pleasance *et al.*, 2010). In addition, melanoma heterogeneity can result from differential expression, in melanoma subsets, of molecules, such as receptor tyrosine kinases (RTKs) affecting relevant intracellular signaling pathways. One of these receptors, Axl, belonging to the TAM (Tyro3, Axl, Mer) family of RTKs, regulates several aspects of tumor biology. Since the initial discovery as a transforming gene (O'Bryan *et al.*, 1991), Axl activation and/or overexpression has been reported in human tumor cells of different histotypes, and evidence for a role in mediating tumor cell invasion and metastasis is continuously increasing (Linger *et al.*, 2010). In melanoma, *Axl* was initially identified in a subset of cell lines through a complementary DNA cloning strategy of transcripts with a protein kinase catalytic domain (Quong *et al.*, 1994). Although subsequently found in two expression signatures of invasiveness (Bittner *et al.*, 2000; Hoek *et al.*, 2006), the single study that addressed its functional role in increasing survival and resistance to apoptosis (van Ginkel

[1]*Unit of Immunobiology of Human Tumors, Department of Experimental Oncology and Molecular Medicine, Fondazione IRCCS Istituto Nazionale dei Tumori, Milan, Italy;* [2]*Unit of Molecular Therapies, Department of Experimental Oncology and Molecular Medicine, Fondazione IRCCS Istituto Nazionale dei Tumori, Milan, Italy;* [3]*Laboratory of Internal Medicine, Department of Clinical and Experimental Medicine, University Amedeo Avogadro of Piemonte Orientale, Novara, Italy and* [4]*Department of Pathology, Fondazione IRCCS Istituto Nazionale dei Tumori, Milan, Italy*

[5]*Current address: Center for Regenerative Therapies, Dresden, Germany*

[6]*Current address: Parc Recerca Biomèdica de Barcelona, Barcelona, Spain*

Correspondence: Marialuisa Sensi or Andrea Anichini, Unit of Immunobiology of Human Tumors, Department of Experimental Oncology and Molecular Medicine, Fondazione IRCCS Istituto Nazionale dei Tumori, Via Venezian 1, Milan 20133, Italy. E-mail: marialuisa.sensi@istitutotumori.mi.it or andrea.anichini@istitutotumori.mi.it

Abbreviations: Axl^{pos}, Axl positive; Axl^{neg}, Axl negative; CM, conditioned medium; MDA, melanocyte differentiation antigen; MITF, microphthalmia transcription factor; RTK, receptor tyrosine kinase; TAM, Tyro3, Axl, Mer

Received 28 December 2010; revised 28 May 2011; accepted 4 June 2011; published online 28 July 2011

© 2011 The Society for Investigative Dermatology

et al., 2004) concerned a uveal tumor. Therefore, for cutaneous melanoma, no information is so far available on the expression, at the protein level, of Axl and its ligand, the vitamin K-dependent gamma-carboxylated protein Gas6 (Varnum *et al.*, 1995), nor on their biological role. In contrast, Tyro3, also belonging to the TAM family, has been identified as a positive regulator of microphthalmia transcription factor (MITF), the ''master regulator of the melanocyte lineage'' in this tumor histotype (Zhu *et al.*, 2009). As MITF expression is associated with higher proliferation but low invasive potential (Bittner *et al.*, 2000; Carreira *et al.*, 2006; Hoek *et al.*, 2006; Segura *et al.*, 2009), we hypothesized that Axl and Tyro3 could contribute to distinct biological behavior. Here, we show that Axl expression is a biomarker for the subset of MITF-negative, melanocyte differentiation antigen (MDA)-negative human melanomas. In agreement, Axl and Tyro3 were found to be mutually exclusive. At the functional level, Axl promoted tumor cell migration and invasion. In this subset of tumors, silencing of endogenous Axl expression or treatment with the Axl-specific inhibitor R428 (Rigel, San Francisco, CA; Holland *et al.*, 2010) reduced their invasive and migratory ability.

RESULTS

Axl is expressed in a subset of primary and metastatic melanoma cell lines

Axl mRNA levels were determined by real-time PCR in 30 of the 58 melanoma cell lines used in this study (Supplementary Table S1 online for tumor origin and mutational status). As shown in Figure 1a, 13/30 (43%) had detectable *Axl* transcripts. A representative western blot, shown in Supplementary Figure S1 online, indicates complete concordance between mRNA and protein expression. Cumulative western blot results for all tumors indicated that Axl was detectable in 22/58 melanoma cell lines (38%), including 3/10 (30%) primary tumors and 19/48 (40%) metastases of different origins (11/35 lymphnodal, 6/11 cutaneous and 2/2 visceral; Supplementary Table S1 online, in red). The two cell lines of normal melanocytes tested lacked Axl expression at the mRNA (Figure 1a) and protein levels (data not shown). In our tumor panel, $BRAF^{V600E}$ and $NRAS^{Q61R}$ mutations occurred in 63.5% and 19% of tumors, respectively (Figure 1b, left-most histogram and Supplementary Table S1 online). Axl expression was significantly more frequent among *NRAS*-mutated melanomas ($P=0.0155$). Indeed, 70% of

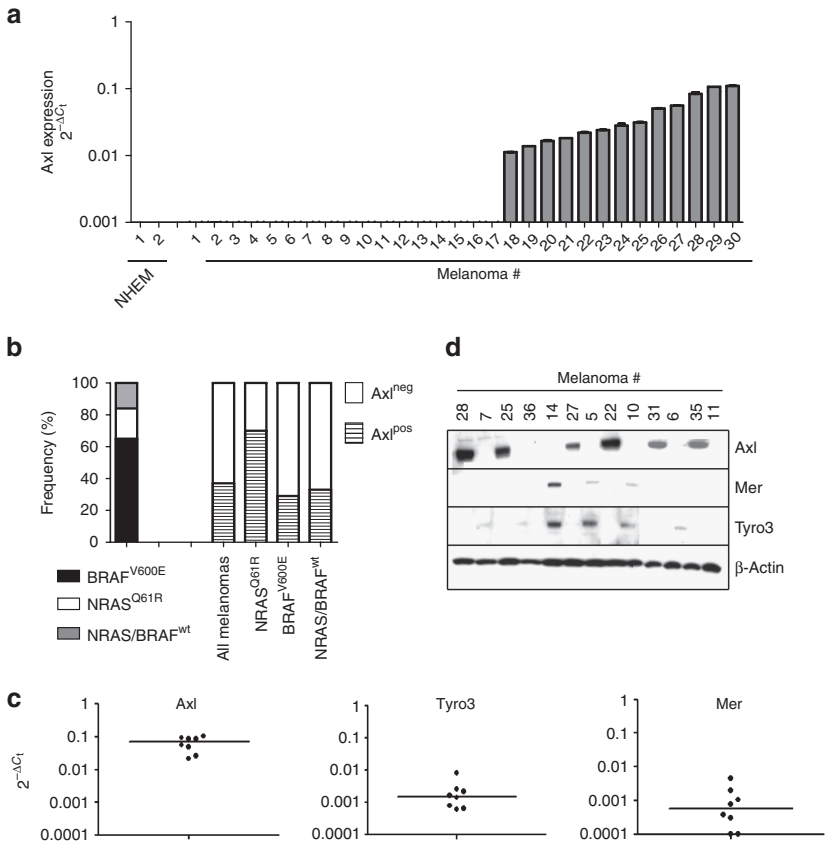

Figure 1. Expression of TAM RTKs in human melanoma lines and frequency distribution of Axl among tumors with different mutational status. (**a**) Axl mRNA levels were measured by real-time PCR in melanoma and human melanocyte lines (NHEM). Data are expressed as $2^{-\Delta C_t}$, where ΔC_t indicates CT (Axl)−CT (β-actin). (**b**) Left-most column: frequency distribution of genetic alterations in the 58 human melanoma cell lines; right columns: frequency distribution of Axl in these melanomas, in the $NRAS^{Q61R}$ or $BRAF^{V600E}$ subsets, and in melanomas negative for these mutations. Axl, Tyro3, and Mer expression measured by (**c**) real-time PCR with data presented as $2^{-\Delta C_t}$, where ΔC_t indicates CT (target gene)−CT (β-actin); (**d**) immunoblot analysis where β-actin expression was used as a loading control. Molecular sizes of Axl, Mer, Tyro3, and β-actin were, respectively, 140, 170, 120, and 42 kDa. Axl^{neg}, Axl negative; Axl^{pos}, Axl positive; NHEM, normal human epidermal neonatal melanocyte; RTK, receptor tyrosine kinase; TAM, Tyro3, Axl, Mer; wt, wild type.

the *NRAS*^{Q61R} mutant tumors were Axl positive (Axl^{pos}), compared with only 29% of *BRAF* mutant and 33% of tumors wild type for these mutations (Figure 1b, right histograms). Real-time PCR on eight Axl^{pos} tumors indicated that transcripts corresponding to *Mer* and *Tyro3*, the other two members of the TAM family of RTK (Figure 1c), were barely expressed. Western blot analysis on representative melanoma cell lines confirmed mutual exclusion of Axl and Tyro3 ($P = 0.047$; Figure 1d). Instead, Mer and Tyro3 were frequently coexpressed on the same tumors.

Melanoma cells express Gas6, which causes Axl phosphorylation

Stimulation of serum-starved melanoma (Me)#28 with exogenously added human rGas6 (1 μg ml^{-1}) led to a time-dependent increase in Akt phosphorylation (Figure 2a), indicating that the receptor was functional. All subsequent experiments were conducted using 500 ng ml^{-1} of rGas6, the minimal amount required for optimal stimulation to occur (Figure 2a), and a stimulation period of 30 minutes. Phosphorylation of extracellular signal-regulated kinase 1/2 was instead not affected by rGas6 (data not shown). rGas6-induced Akt phosphorylation was greatly reduced by preincubation with Axl/Fc-soluble recombinant protein (Figure 2a), confirming the specificity of the interaction. Immunoprecipitation of tyrosine-phosphorylated proteins, followed by immunostaining for Axl, evidenced a basal Axl phosphorylation in cell lysates of unstimulated serum-starved Me#28 cells that increased following stimulation with rGas6 (Figure 2b). Basal Axl phosphorylation suggested that Axl^{pos} melanomas could endogenously produce the Axl ligand Gas6. In agreement, as determined by specific ELISA, 48 hour-conditioned medium (CM) from 57% Axl^{pos} melanoma lines contained detectable Gas6 (>1 ng ml^{-1}; Figure 2c). In addition, several of these tumors secreted Gas6 at levels comparable to or even higher than WI-38, the reference line for Gas6 production (Varnum *et al.*, 1995; Figure 2c). These results suggested that, in a consistent fraction of tumors, ligand activation of Axl could occur not only by a paracrine but also by an autocrine mechanism. To prove that Gas6 produced by melanoma cells was able to phosphorylate Axl receptor, serum-starved Me#28 cells were stimulated for 30 minutes with CM from WI-38 and Me#25 or from Me#24 (no Gas6 production) as negative control. As vitamin K-dependent γ-gutamyl carboxylation of Gas6 is necessary for its biological activity, CM was produced in serum-free medium supplemented with 10 μg ml^{-1} of vitamin K. In order to obtain a higher amount of Gas6, 5 days of *in vitro* culture in these conditions was carried out. As shown in Figure 2d, addition of CM from Me#25 and WI-38, equivalent to 100 ng of endogenous Gas6, but not from Me#24, resulted in Axl phosphorylation as detected by ELISA. This effect was specific as it was abrogated by the addition of Axl/Fc. These results indicate that melanoma cells can produce biologically active carboxylated Gas6. As shown in Figure 3a, Axl^{pos} melanomas producing Gas6 at high (Me#20 and 25) or intermediate (Me#27, and 28) levels display the presence of cell-bound Gas6, indicative of

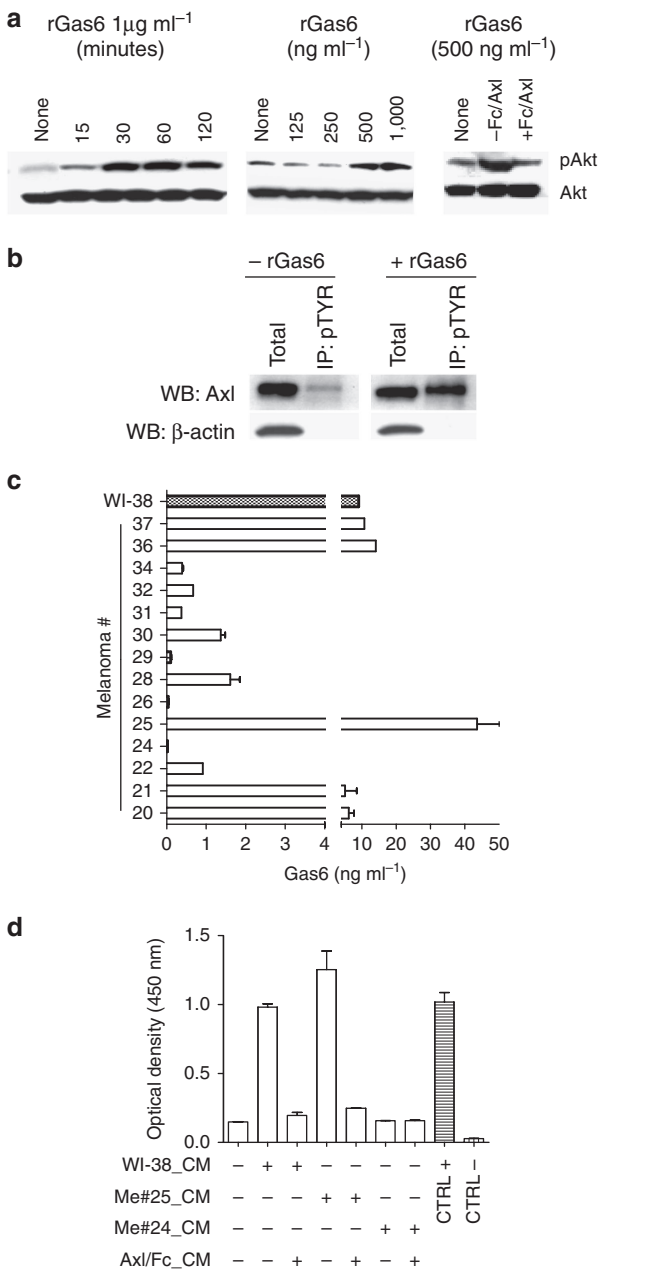

Figure 2. Axl activation and autocrine production of Gas6. (**a**) Immunoblot of Akt and pAkt (both 57 kDa) on lysates from Me#28 stimulated for specified times and doses with rGas6 with or without 1 hour pretreatment with Axl/Fc (2.5 μg ml^{-1}). (**b**) Phosphorylated Axl expression in Me#28, either untreated (−rGas6) or stimulated with rGas6 (500 ng ml^{-1} for 30 minutes). Cell lysates were immunoprecipitated with anti-phosphotyrosine antibody 4G10 and immunoblotting was performed with anti-Axl. (**c**) ELISA quantification of Gas6 levels in CM taken from confluent cultures of melanomas (empty bars) or from WI-38 (filled bar). Means ± SD from two to four detections are shown. (**d**) ELISA quantification of Axl phosphorylation in lysates of Me#28 treated for 30 minutes with CM from WI-38, Me#25 or Me#24, or with either CM preincubated for 1 hour with Axl/Fc. CTRL^{-}, no lysate; CTRL^{+}, recombinant human phosphorylated Axl (2 ng ml^{-1}). CM, conditioned medium; CTRL, control; IP, immunoprecipitation; pAkt, Akt phosphorylation; pTYR, phosphorylated tyrosines; WB, western blotting.

Axl/Gas6 interaction (Gjerdrum *et al.*, 2010). Tumors that do not secrete Gas6 (Me#14, Axl negative, Axl^{neg}), even if Axl^{pos} (as Me#24), are negative for surface expression of Gas6.

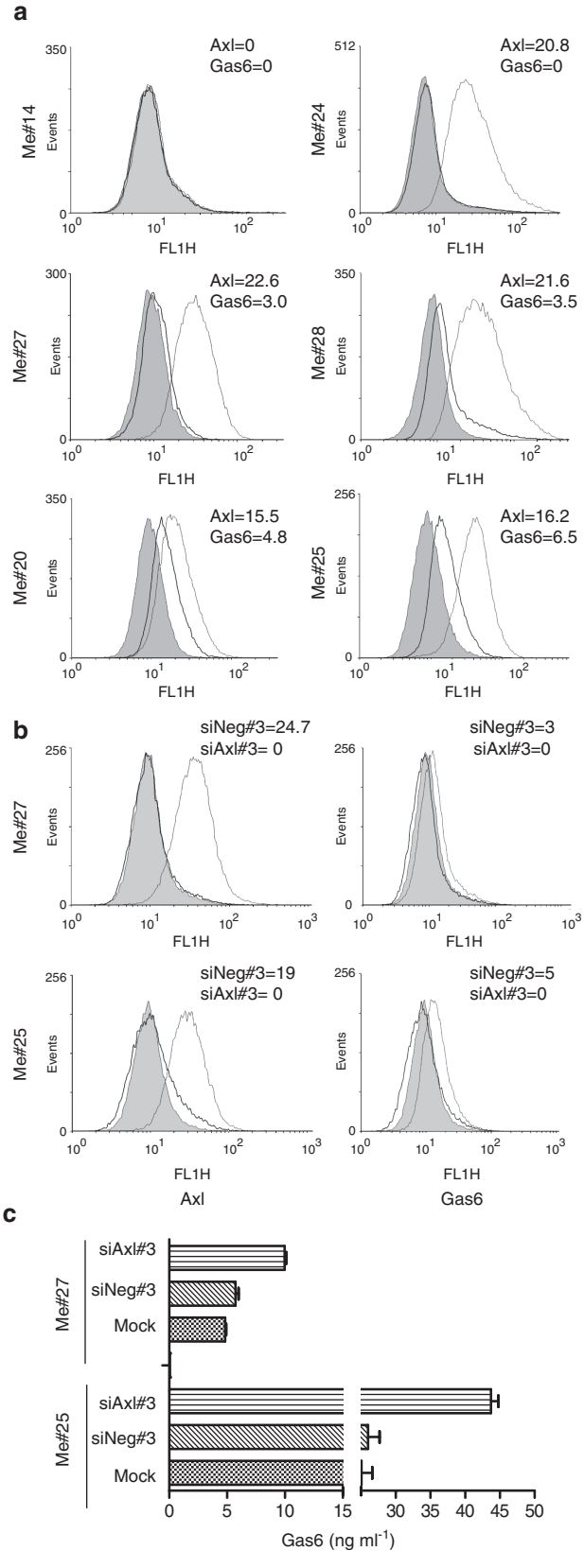

Axl knockdown by transient transfection of a Stealth small interfering RNA (siRNA) (Invitrogen, Paisley, UK) to Axl (siAxl#3) reduced Axl protein levels by more than 99% 48 hr after transfection (Figure 3b). As a consequence, cell-bound Gas6 could no longer be detectable (Figure 3b) and, conversely, increased Gas6 secretion occurred in conditioned media (Figure 3c). A non-silencing siRNA (siNeg#3) had no effect on Axl and on cell-surface-bound Gas6 expression (Figure 3b).

Computational analysis in published melanoma data sets

Pearson's correlation analysis of five data sets, containing expression profiles of 166 melanoma lines (Pavey *et al.*, 2004; Hoek *et al.*, 2006; Wagner *et al.*, 2007; Supplementary Table S2 online), yielded 256 genes the expression of which correlated negatively (Supplementary Table S3 online) or positively (Supplementary Table S4 online) with *Axl* in all data sets, with a *P*-value <0.05 and a Pearson correlation coefficient (r) exceeding 0.4. Functional analysis of negatively (112) or positively (144) correlated genes (see Supplementary Tables S5 and S6 online) was carried out by Ingenuity Pathway Analysis (IPA; http://www.ingenuity.com). The top three functions, associated with the highest score network of negatively correlated genes, were ''Amino acid metabolism'', ''Hair and skin development and function'', and ''Small molecule biochemistry'' (Supplementary Table S7 online). As shown in Figure 4a, central to this network is *MITF*, the master regulator of melanocyte development, differentiation, and survival (Mitra and Fisher, 2009). In accordance, 65% (72/110, see Supplementary Table S5 online, column 5) of negatively correlated genes overlap with MITF-regulated genes (Hoek *et al.*, 2008b), like those encoding well-known MDAs such as MART-1 (*MLANA*), gp100 (*SILV*), tyrosinase (*TYR*), tyrosinase-related protein 1 (*TYRP1*), and dopachrome tautomerase (*DCT*) (Mitra and Fisher, 2009). In addition, ''Pigmentation'' and ''Melanocyte development and pigmentation signaling'' were, respectively, the top biological functions and canonical pathways (Supplementary Table S7 online). Forty percent (44/112) of *Axl*-negatively correlated genes are included in gene signatures of melanoma cell lines with low metastatic potential (Supplementary Table S5 online, columns 6–8; Hoek *et al.*, 2006; Jeffs *et al.*, 2009). Within the set of

Figure 3. Cell-bound Gas6 expression in Axl^{pos} melanomas. (**a**) Surface staining of Axl and Gas6 as detected by flow cytometry in six different melanoma cell lines. Gray histograms, staining with isotype control antibodies; dotted histograms, Axl expression; and bold histograms, Gas6 expression. (**b**) Axl knockdown abrogates cell-associated Gas6. Gray histograms, staining with isotype control antibodies; bold histograms, expression of Axl (left) or Gas6 (right) in Me#25 and 27 cells transfected with siAxl#3; and dotted histograms, expression of Axl (left) or Gas6 (right) in Me#25 and 27 cells transfected with siNeg#3. (**c**) Increased Gas6 secretion in CM from Axl-knockdown compared with parental and siNeg#3 Me#25 and 27 transfected cells as detected by ELISA. The numbers in histograms refer to MFI for Axl or Gas6 after subtraction of MFI of isotype control. Axl^{pos}, Axl positive; CM, conditioned medium; MFI, median fluorescence intensity.

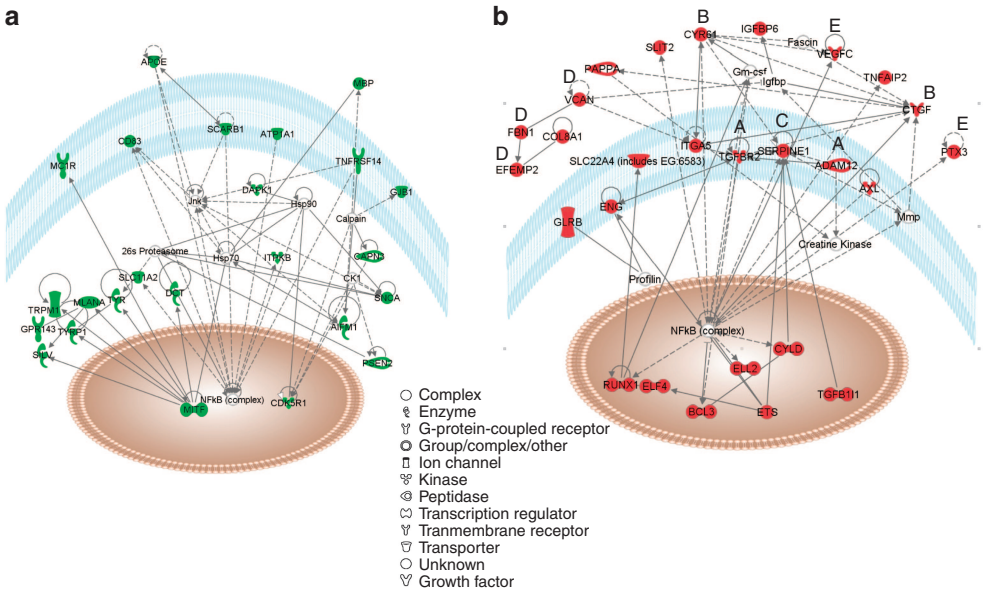

Figure 4. Graphical representation of the top score networks identified by IPA. Molecular relationships between genes correlating negatively (**a**, in green) or positively (**b**, in red) with Axl. Molecules and functions in networks: (A) local environment; (B) ECM interactions; (C) ECM modeling; (D) main ECM components; and (E) secreted factors. ECM, cell–extracellular matrix; IPA, Ingenuity Pathway Analysis. Gene names corresponding to gene symbols are listed in Supplementary Tables S5 and S6 online.

positively correlated genes, the top IPA network was associated with ''Cellular movement, Cell-to-cell signaling, and interaction and Tissue development'' and the top IPA functions were ''Migration'' and ''Invasion'' of eukaryotic cells (Supplementary Table S7 online). One-fourth of *Axl*-positively correlated genes are included in gene signatures of melanomas with high metastatic potential (Hoek *et al.*, 2006; Jeffs *et al.*, 2009; Supplementary Table S6 online, column 5–7).

AXL as a determinant of invasion and motility for MITF-negative melanomas

Computational analysis predicted a prominent expression of Axl RTK among poorly differentiated melanomas characterized by a lack of expression of MITF and MDAs (Figure 4a), but displaying, in accordance with the known role of Axl in regulating invasive ability (Linger *et al.*, 2010), high expression of motility-related genes and ability to engage extensive cross-talk with the stromal and extracellular microenvironment (Figure 4b). Flow cytometry, performed on 10 Axl^{pos} and 9 Axl^{neg} melanoma cell lines, confirmed the highly significant association of MART-1 and gp100 expression with Axl^{neg} tumors (Figure 5a). The cancer testis antigen MAGE-1, an antigen not belonging to the MDA class and not MITF regulated (Zendman *et al.*, 2003), was instead expressed equally on both subsets (Figure 5a). In addition to MART-1, western blot analysis confirmed that MITF could only be detected in Axl^{neg} tumors (Figure 5b, for representative results). Immunohistochemical evaluation of Axl protein levels in tissue sections from melanoma lesions (Figure 5c for overall results) indicated that 86% of the lesions were either Axl^{neg}MITF^{pos} (57%) or Axl^{pos}MITF^{neg} (29%). Two lesions displayed a mixed Axl^{pos}MITF^{pos} profile, although we cannot rule out expression of the two markers in different cells. Representative staining of two Axl^{pos} MITF^{neg} melanomas (Figure 5d, patients no. 1 and 2) and of two Axl^{neg}MITF^{pos} tumors (Figure 5D, patients no. 3 and 4) is shown. In agreement with the tissue distribution of Axl (Holland *et al.*, 2005; Ye *et al.*, 2010), staining of endothelial cells could be observed, even when neoplastic cells were Axl^{neg} (Figure 5d, patient no. 4). Supplementary Figure S2 online shows staining of the same vascular structures by anti-CD31 and anti-Axl. Axl expression positively and significantly correlated with the ability of different cell lines to migrate and invade matrigel *in vitro* (Figure 6a). Axl silencing by siAxl#3 and/or by a different Stealth siRNA (siAxl#2) suppressed Axl protein expression and Akt phosphorylation by rGas6 (500 ng ml^{-1}) in Me#28 cells (Figure 6b). Real-time PCR performed on RNA from siAxl#3 Axl-silenced cells on day 11 of Axl knockdown did not reveal, in comparison with siNeg#3 control cells, changes in transcript levels of *MITF* and *MART-1*, whereas Axl was downregulated 22-fold (Supplementary Figure S3a online). No MITF or MART-1 protein re-expression was also observed by western blot analysis up to 14 days of Axl knockdown (Supplementary Figure S3b online). Invasive or migratory behavior of Me#28 *in vitro* in response to 10% fetal calf serum was instead reduced (Figure 6c) by 50% and 40%, respectively, by Axl knockdown. As shown in Supplementary Figure S4a online, diminished invasive behavior could not be explained by decreased cell proliferation. Axl-silenced Me#28 cells were also impaired when compared with control cells at closing a wound (Figure 6d and e) and at migrating through a confluent human umbilical vein

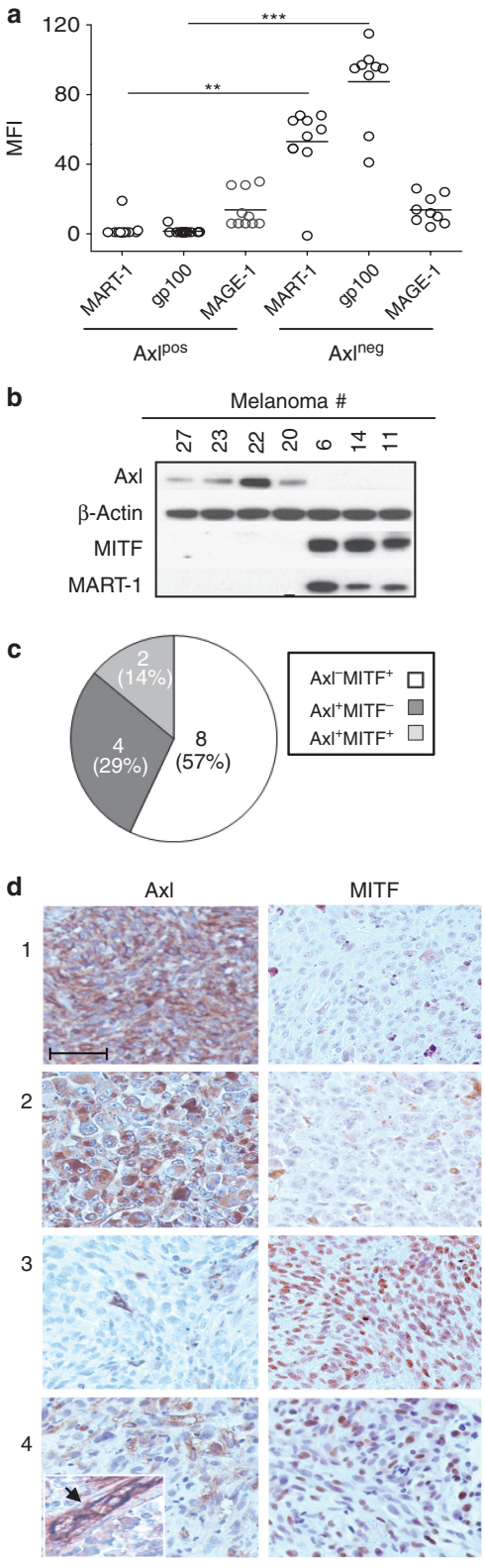

endothelial cell monolayer (Figure 6f). Treatment with R428, a newly described selective small-molecule inhibitor of Axl tyrosine kinase activity (Holland *et al.*, 2010), used at 2 μM, a drug concentration that did not affect cell proliferation (Supplementary Figure S4b online), was effective in reducing wound closure (Figure 6g), migration (Figure 6h), and invasion (Figure 6i) of Me#28 at levels comparable to those achieved by siRNA-mediated Axl knockdown.

DISCUSSION

The results of the present study indicate that Axl is a molecular biomarker for human melanomas lacking MITF (Mitra and Fisher, 2009), as well as of MITF-regulated MDAs. In this subset of tumors, we found that Axl has a role in the regulation of motility and invasion. A high proportion (57%) of Axl^{pos} melanoma cell lines also secreted the Axl ligand Gas6 in a biologically active form. In addition, Axl and Gas6 were significantly correlated (P-value <0.05 and a Pearson correlation coefficient exceeding 0.4) in four out of five analyzed melanoma data sets, confirming the relevance of the autocrine loop, active also in other tumor histotypes (Linger *et al.*, 2010), for Axl signaling. In our panel of melanoma lines, Axl protein was more frequently associated with $NRAS^{Q61R}$ compared with $BRAF^{V600E}$ mutant melanomas or with tumors wild type for these mutations (Figure 1b, right histograms), a finding that needs to be validated in a larger cohort of tumors. Lack of expression of Tyro3, the other TAM family member recently shown to function as a positive regulator of MITF in melanoma (Zhu *et al.*, 2009), by Axl^{pos} tumors (Figure 1c and d) is consistent with the two major expression signatures of human melanoma cell lines that define the invasive versus proliferative phenotype (Hoek *et al.*, 2006). In this framework, Axl appears to define the class of undifferentiated melanomas with higher motility/invasive ability, whereas Tyro3, shown to regulate the proliferation rate of melanomas harboring such a receptor (Zhu *et al.*, 2009), can define more differentiated tumors characterized by increased proliferation. MART-1 and MITF were not induced by up to 14 days of Axl knockdown in our model system (Supplementary Figure S3 online). Further investigations will be needed to elucidate the molecular events that govern the inverse relationship between MITF and Axl expression levels. Immunohistochemical staining confirmed the reciprocal expression of these two markers, but also evidenced lesions positive for both. The latter finding is

Figure 5. Expression of Axl is inversely correlated to that of MITF and MDAs. (**a**) MART-1, gp100, and MAGE-1 expression levels were examined by flow cytometry across a set of 10 Axl^{pos} and 9 Axl^{neg} melanoma samples. Isotype antibody was used as negative control. (**b**) Immunoblot analysis of Axl (140 kDa), MITF (54 kDa), and MART-1 (17 kDa). β-Actin (42 kDa) was used as a loading control. (**c**) Summary of immunohistochemical staining for Axl and MITF in melanoma specimens. (**d**) Staining for MITF and Axl in representative primary melanomas (#1–4). Me#4 is highly vascularized, and anti-Axl antibody stains endothelial cells as shown at higher magnification in the inset (arrow) and in Supplementary Figure S2 online. Bar = 50 μm. Axl^{neg}, Axl negative; Axl^{pos}, Axl positive; MFI, median fluorescence intensity; MITF, microphthalmia transcription factor. $^{**}P<0.01$, $^{***}P<0.001$.

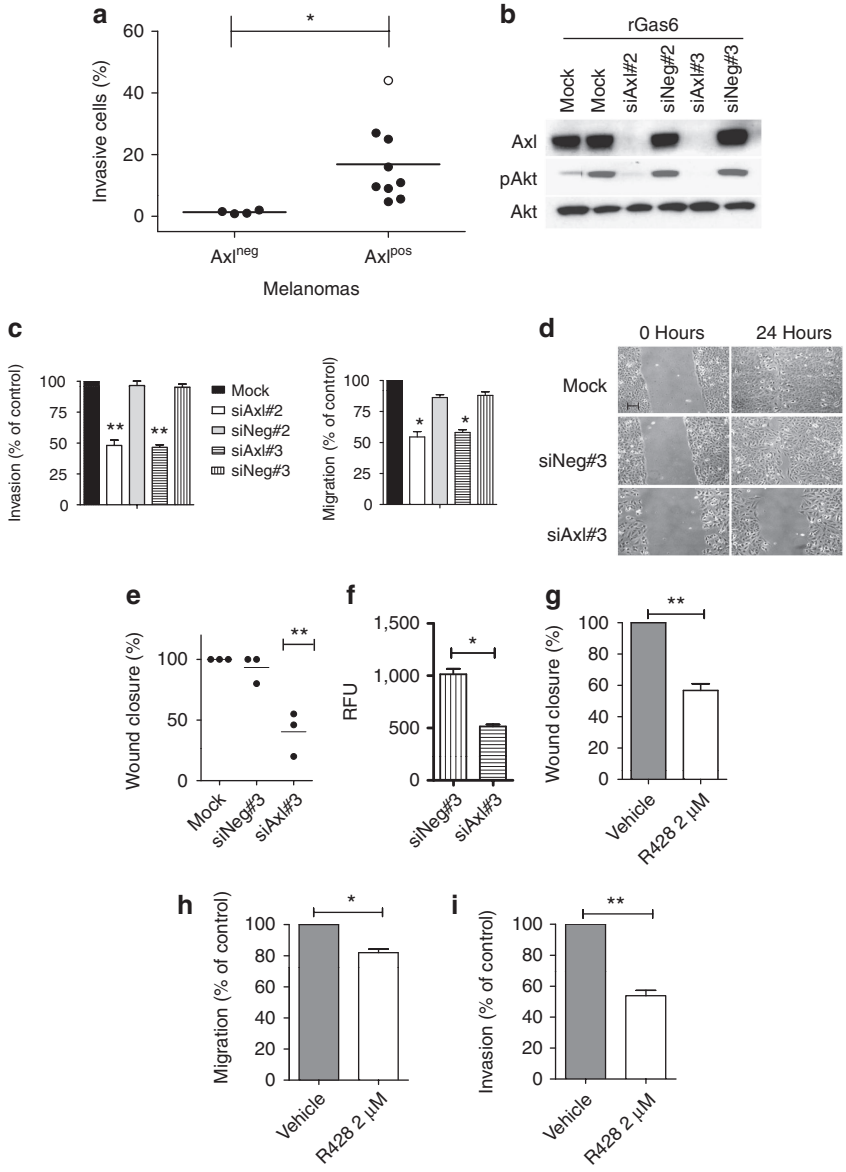

Figure 6. Relevance of Axl expression in motility and invasivity of human melanoma cells. (**a**) Invasion of Axl^{pos} and Axl^{neg} melanomas toward medium containing 10% FBS. The number of invading cells is reported as a percentage of seeded cells. White circle = Me#28. (**b**) Immunoblot of Axl, Akt, and pAkt in Axl-knockdown (siAxl#2, #3) or control (mock and siNeg#2, #3) Me#28 cells stimulated for 30 minutes with 500 ng ml^{-1} rGas6. (**c**) Invasion, migration, and (**d**) wound healing of Axl-knockdown Me#28 cells in comparison with mock-transfected cells. Bar = 200 µm. (**e**) Wound closure of three different Axl-knockdown or control melanomas. (**f**) Migration of Axl-knockdown or control Me#28 cells through a HUVEC endothelial layer. Results are expressed as RFU values of migrated cells. (**g**) Wound healing, (**h**) migration, and (**i**) invasion of Me#28 in the presence of R428 (2 µM) or vehicle (0.25% DMSO). Axl^{neg}, Axl negative; Axl^{pos}, Axl positive; FBS, fetal bovine serum; HUVEC, human umbilical vein endothelial cell; pAkt, Akt phosphorylation; RFU, relative fluorescence unit. *$P<0.05$, **$P<0.01$.

in accordance with the phenotype switch model predicting that gene expression programs of neoplastic cells can be regulated by the cellular microenvironment (Hoek *et al.*, 2008a). Thus, according to the type of microenvironment, tumor cells may switch between the invasive phenotype (i.e., a condition more likely to require Axl expression) and the proliferative phenotype (i.e., a condition that does not necessarily require Axl expression). Support for this model comes not only from published observations (Hoek and Goding, 2010) but also from our own preliminary results (data not shown). We indeed found that subcutaneous tumor nodules and pulmonary metastases (after intravenous tumor injection) isolated from severe combined immunodeficient mice injected with Axl^{pos} melanoma cells were characterized by strong downregulation of Axl. The same receptor was, however, re-expressed upon brief *in vitro* culture of these nodules or pulmonary metastases. Finally, the results of this study suggest that Axl-directed therapies may be developed in MITF-negative melanomas. As a proof of concept, we used R428, a selective small-molecule inhibitor

of Axl tyrosine kinase activity recently shown to improve survival and reduce metastatic burden in mouse models of breast cancer (Holland *et al.*, 2010). R428 significantly interfered with mechanisms of migration and invasion of Axl^{pos} melanoma cells at levels comparable to Axl knockdown. The greater efficacy of Axl inhibition (by both siRNA and R428) in reducing invasion compared with migration could be related to Axl-dependent expression of matrix-degrading enzymes as described (Tai *et al.*, 2008). Our results, together with the recent identification of Axl among a number of kinases that might drive melanoma resistance to BRAF kinase inhibitor PLX4032 (Johannessen *et al.*, 2010; Wagle *et al.*, 2011), further strengthen the possible relevance of Axl inhibition in a clinical setting.

MATERIALS AND METHODS

Cell lines and reagents

Primary and metastatic melanoma cell lines were established *in vitro* from surgical specimens removed from patients admitted to our Institution and were cultured in RPMI medium (Lonza, Basel, Switzerland) as described (Anichini *et al.*, 1996). The study was conducted according to the Declaration of Helsinki Principles and institutional approval for experiments was not required. Written informed consent was obtained from patients. Molecular and biological characterization of these cell lines has been reported previously (Daniotti *et al.*, 2004). Short-term cultures not exceeding 10–15 passages were used. The human lung fibroblast cell line WI-38 (ATCC, LGC Standards, Milano, Italy), normal human epidermal neonatal melanocytes, and human umbilical vein endothelial cells (both from PromoCell, Heidelberg, Germany) were cultured according to the manufacturer's instructions. All lines were tested for the absence of mycoplasma contamination by Hoechst 33258 (Sigma-Aldrich, St Louis, MO). Primary antibodies used are listed in Supplementary Table S8 online. The Axl inhibitor R428 was provided by Rigel. It was dissolved in DMSO (10 mM). DMSO final concentration in the assay media was 0.25%.

Flow cytometry

Melanoma cells, permeabilized or not (for cytoplasmic and surface staining), were stained by sequential incubation with primary and secondary mAbs as described (Sensi *et al.*, 2005, 2009). Cells were analyzed for antigen expression by a FACSCalibur cytofluorimeter (Becton Dickinson, Franklin Lakes, NJ). Percentage of positive cells and median fluorescence intensity after background subtraction were recorded.

Real-time PCR

Axl (Hs00242357-m1), *Tyro3* (Hs00170723-m1), *Mer* (Hs00179024-m1), *MITF* (Hs00165156-m1), and *MART-1* (Hs00194133-m1) TaqMan Gene expression assays (Applied Biosystems, Foster City, CA) have been used. *β-Actin* (433762F) served as endogenous control. Total RNA (2 μg) extracted from the different melanoma cell lines was reverse transcribed using a QuantiTect Reverse Transcription kit (Qiagen, Venlo, The Netherlands). Preliminary experiments were conducted for the internal control gene (*β-actin*) using the C_t slope method to ensure that the quality of each complementary DNA and the dynamic range of amplifications were comparable (Schmittgen and Livak, 2008). Real-time PCR was then carried out with 30 ng input complementary DNA, 1 × TaqMan Gene Expression Master Mix on a ABI PRISM 7900 HT thermal cycler (Applied Biosystems). Data were analyzed using ABI PRISM Sequence Detection Software version 2.2.2 (Applied Biosystems). Relative expression was determined on quadruplicate reactions using the formula $2^{-\Delta C_t}$, reflecting target gene expression normalized to *β-actin* levels (Schmittgen and Livak, 2008). Fold-change modifications of gene expression were obtained using $2^{-\Delta\Delta C_t}$ method (Schmittgen and Livak, 2008).

Western blot

SDS-PAGE was performed using 20 μg protein lysates on NuPage 4–12% Bis-Tris precasted mini-gels (Invitrogen, Paisley, UK) in MOPS buffer (Invitrogen). Proteins were transferred onto PVDF membranes (Hybond-P, GE Healthcare, Little Chalfont, UK) using NuPage Transfer Buffer, without methanol. Development was carried out by the chemiluminescence method with the ECL Plus Western Blotting Detection System (GE Healthcare) and autoradiography.

Production of CM and Gas6 quantification

Cells were grown in 100 mm cell culture dishes (Corning, Corning, NY) in medium supplemented with 10 μg ml^{-1} vitamin K (Konakion, Roche, Basel, Switzerland). At subconfluence, the medium was substituted with the corresponding serum-free medium. CM was recovered after 48 hours or after 5 days (for functional assays). Secreted Gas6 was quantified by ELISA as described (Alciato *et al.*, 2008).

Axl phosphorylation

After an overnight starvation, subconfluent melanoma cells were treated for 30 minutes with serum-free medium containing 500 ng ml^{-1} of recombinant Gas6 (R&D Systems, Abingdon, UK) or with CM. In some experiments, recombinant human Axl/Fc chimera at 2.5 μg ml^{-1} (R&D Systems) was added for 1 hour before the addition of rGas6 or CM. Axl phosphorylation was then measured by DuoSet IC ELISA (R&D Systems) using 250 μg of protein lysate. Data were expressed as 450 nm optical density. Immunoprecipitation and immunoblotting were performed as described (De Santis *et al.*, 2009).

Axl knockdown

Stealth siRNA duplexes, specific for *Axl* and negative controls (Supplementary Table S9 online), were used (10 nM final concentration) according to Lipofectamine RNAiMax guidelines (Invitrogen).

Migration and invasion assays

Cells maintained for 24 hour in serum-free medium were harvested and transferred to the upper chamber (1.5×10^5cells per well) of uncoated (migration) or matrigel-coated (invasion) 24-well chambers (8 μm pore size, QCM 24-well Fluorimetric Assay kit, Millipore, Billerica, MA). RPMI medium containing 10% fetal bovine serum was added to the lower chamber. R428 (2 μM) or vehicle (DMSO, 0.25%) was added for 2 hours to cells before loading them in the upper chambers. Both the upper and lower chambers contained the drug or vehicle. Quantification of migrating/invading cells was obtained by measuring their fluorescent signals with a 480/520 nm filter set on an Infinite M1000 microplate reader (Gentronix, Manchester, UK) 20 or 42 hours later, respectively.

Scratch wound migration assay

Confluent cultures were wounded using a sterile 200 µl pipette tip. Where indicated, wounds were made in the presence of R428 (2 µM) or vehicle (DMSO, 0.25%). Wound closure was assessed 24 hours later using an Axiovert 100 microscope with a 5× PanFluor objective, and images were acquired with the AxioVision System (Carl Zeiss, Thornwood, NY). Data are expressed as a percentage of wound closure of the original wound width.

Transendothelial migration assay

Melanoma cells were marked with CytoTracker (Invitrogen), plated in serum-free RPMI onto a human umbilical vein endothelial cell monolayer in the upper inserts of invasion chambers, and allowed to transmigrate through the endothelium and the membrane for 24 hour according to the instructions given in the CytoSelect Tumor Transendothelial Migration Assay Kit (Cell Biolabs, San Diego, CA). Non-migratory cells were removed, migratory cells were lysed, and their fluorescence was determined with the Infinite M1000 microplate reader (Gentronix) at 480/520 nm. Results are indicated as relative fluorescence units.

Immunohistochemistry

Formalin-fixed and paraffin-embedded tissue staining was performed as described previously (Sensi *et al.*, 2005). Images were acquired using an Axiovert 100 microscope with the Axiovision System using ×20 magnification (Carl Zeiss).

Computational analysis

Five melanoma cell line data sets, all arrayed on Affymetrix platforms, were downloaded from the NCBIs Gene Expression Omnibus (http://www.ncbi.nlm.nih.gov/geo/; Pavey *et al.*, 2004; Hoek *et al.*, 2006; Wagner *et al.*, 2007). All probe sets were collapsed to gene symbols on the basis of Affymetrix, Santa Clara, CA annotations. Pearson's correlation coefficients were calculated between expression measurements of Axl and those of the remaining genes across all samples of each data set using the cor function from the R Stats package (http://stat.ethz.ch/R-manual/R-patched/library/stats/html/00Index.html). *P*-values for correlation coefficients were determined according to the method described by Graeber and Eisenberg (2001) using an in-house script in R language (http://www.r-project.org/). Briefly, expression values for gene *Axl* were randomly permuted (10,000 times) and correlation coefficients between permuted *Axl* expression and expression data for the remaining genes in the data set were calculated. In this way, the distribution of correlation coefficients under the null hypothesis was obtained, allowing computation of the permutation *P*-value, testing whether the correlation coefficient equals zero. Assuming ρ is the observed correlation coefficient between *Axl* and gene *B*, the two-tailed *P*-values were obtained as the proportion of permuted correlation coefficients with values larger than ρ or smaller than $-\rho$. IPA 8.5 was used to analyze the signaling pathways, cellular location, function, and network connections of the identified genes. Further details are given in Supplementary Information online.

Statistical analysis

Analysis of variance, followed by an Student-Newman-Keul multiple comparison test or a one-sample *t*-test to a theoretical value, have been used for significance evaluation. Correlation of *Axl* expression with mutations affecting *NRAS* or *BRAF*, as well as with *Tyro3* expression, was analyzed by Fisher's exact test. All statistical tests were conducted using GraphPad Prism 5 (GraphPad Software, La Jolla, CA). Asterisks indicate $*P<0.05$, $**P<0.01$, and $***P<0.001$.

CONFLICT OF INTEREST

The authors state no conflict of interest.

ACKNOWLEDGMENTS

We thank Mrs Alessandra Molla, Mrs Claudia Vegetti, and Dr Alberto Zacchetti for excellent technical assistance. We also thank Dr Sacha Holland and Rigel for providing the specific Axl kinase inhibitor R428 and for communication and information pertaining to its usage. This investigation was supported by Fondazione CARIPLO (2008-2411), Alleanza contro il Cancro, Ministero della Salute (AA), and AIRC (AA and SC).

SUPPLEMENTARY MATERIAL

Supplementary material is linked to the online version of the paper at http://www.nature.com/jid

REFERENCES

Alciato F, Sainaghi PP, Castello L *et al* (2008) Development and validation of an ELISA method for detection of growth arrest specific 6 (GAS6) protein in human plasma. *J Immunoassay Immunochem* 29:167–80

Anichini A, Mortarini R, Maccalli C *et al.* (1996) Cytotoxic T cells directed to tumor antigens not expressed on normal melanocytes dominate HLA-A2.1-restricted immune repertoire to melanoma. *J Immunol* 156: 208–17

Bittner M, Meltzer P, Chen Y *et al.* (2000) Molecular classification of cutaneous malignant melanoma by gene expression profiling. *Nature* 406:536–40

Carreira S, Goodall J, Denat L *et al.* (2006) Mitf regulation of Dia1 controls melanoma proliferation and invasiveness. *Genes Dev* 20:3426–39

Curtin JA, Busam K, Pinkel D *et al.* (2006) Somatic activation of KIT in distinct subtypes of melanoma. *J Clin Oncol* 24:4340–6

Daniotti M, Oggionni M, Ranzani T *et al.* (2004) BRAF alterations are associated with complex mutational profiles in malignant melanoma. *Oncogene* 23:5968–77

De Santis G, Miotti S, Mazzi M *et al.* (2009) E-cadherin directly contributes to PI3K/AKT activation by engaging the PI3K-p85 regulatory subunit to adherens junctions of ovarian carcinoma cells. *Oncogene* 28: 1206–17

Gjerdrum C, Tiron C, Hoiby T *et al.* (2010) Axl is an essential epithelial-to-mesenchymal transition-induced regulator of breast cancer metastasis and patient survival. *Proc Natl Acad Sci USA* 107:1124–9

Graeber TG, Eisenberg D (2001) Bioinformatic identification of potential autocrine signaling loops in cancers from gene expression profiles. *Nat Genet* 29:295–300

Hoek KS, Eichhoff OM, Schlegel NC *et al.* (2008a) *In vivo* switching of human melanoma cells between proliferative and invasive states. *Cancer Res* 68:650–6

Hoek KS, Goding CR (2010) Cancer stem cells versus phenotype-switching in melanoma. *Pigment Cell Melanoma Res* 23:746–59

Hoek KS, Schlegel NC, Brafford P *et al.* (2006) Metastatic potential of melanomas defined by specific gene expression profiles with no BRAF signature. *Pigment Cell Res* 19:290–302

Hoek KS, Schlegel NC, Eichhoff OM *et al.* (2008b) Novel MITF targets identified using a two-step DNA microarray strategy. *Pigment Cell Melanoma Res* 21:665–76

Holland SJ, Pan A, Franci C *et al.* (2010) R428, a selective small molecule inhibitor of Axl kinase blocks tumor spread and prolongs survival in models of metastatic breast cancer. *Cancer Res* 70:1544–54

Holland SJ, Powell MJ, Franci C *et al.* (2005) Multiple roles for the receptor tyrosine kinase axl in tumor formation. *Cancer Res* 65:9294–303

Jeffs AR, Glover AC, Slobbe LJ *et al.* (2009) A gene expression signature of invasive potential in metastatic melanoma cells. *PLoS One* 4:e8461

Johannessen CM, Boehm JS, Kim SY *et al.* (2010) COT drives resistance to RAF inhibition through MAP kinase pathway reactivation. *Nature* 468:968–72

Lee JH, Choi JW, Kim YS (2011) Frequencies of BRAF and NRAS mutations are different in histologic types and sites of origin of cutaneous melanoma: a meta-analysis. *Br J Dermatol* 164:776–84

Linger RM, Keating AK, Earp HS *et al.* (2010) Taking aim at Mer and Axl receptor tyrosine kinases as novel therapeutic targets in solid tumors. *Expert Opin Ther Targets* 14:1073–90

Mitra D, Fisher DE (2009) Transcriptional regulation in melanoma. *Hematol Oncol Clin North Am* 23:447–65, viii

O'Bryan JP, Frye RA, Cogswell PC *et al.* (1991) axl, a transforming gene isolated from primary human myeloid leukemia cells, encodes a novel receptor tyrosine kinase. *Mol Cell Biol* 11:5016–31

Palavalli LH, Prickett TD, Wunderlich JR *et al.* (2009) Analysis of the matrix metalloproteinase family reveals that MMP8 is often mutated in melanoma. *Nat Genet* 41:518–20

Pavey S, Johansson P, Packer L *et al.* (2004) Microarray expression profiling in melanoma reveals a BRAF mutation signature. *Oncogene* 23: 4060–7

Pleasance ED, Cheetham RK, Stephens PJ *et al.* (2010) A comprehensive catalogue of somatic mutations from a human cancer genome. *Nature* 463:191–6

Prickett TD, Agrawal NS, Wei X *et al.* (2009) Analysis of the tyrosine kinome in melanoma reveals recurrent mutations in ERBB4. *Nat Genet* 41: 1127–32

Quong RY, Bickford ST, Ing YL *et al.* (1994) Protein kinases in normal and transformed melanocytes. *Melanoma Res* 4:313–9

Schmittgen TD, Livak KJ (2008) Analyzing real-time PCR data by the comparative CT method. *Nat Protoc* 3:1101–8

Segura MF, Hanniford D, Menendez S *et al.* (2009) Aberrant miR-182 expression promotes melanoma metastasis by repressing FOXO3 and microphthalmia-associated transcription factor. *Proc Natl Acad Sci USA* 106:1814–9

Sensi M, Nicolini G, Zanon M *et al.* (2005) Immunogenicity without immunoselection: a mutant but functional antioxidant enzyme retained in a human metastatic melanoma and targeted by CD8(+) T cells with a memory phenotype. *Cancer Res* 65:632–40

Sensi M, Pietra G, Molla A *et al.* (2009) Peptides with dual binding specificity for HLA-A2 and HLA-E are encoded by alternatively spliced isoforms of the antioxidant enzyme peroxiredoxin 5. *Int Immunol* 21:257–68

Tai KY, Shieh YS, Lee CS *et al.* (2008) Axl promotes cell invasion by inducing MMP-9 activity through activation of NF-kappaB and Brg-1. *Oncogene* 3:4044–55

van Ginkel PR, Gee RL, Shearer RL *et al.* (2004) Expression of the receptor tyrosine kinase Axl promotes ocular melanoma cell survival. *Cancer Res* 64:128–34

Varnum BC, Young C, Elliott G *et al.* (1995) Axl receptor tyrosine kinase stimulated by the vitamin K-dependent protein encoded by growth-arrest-specific gene 6. *Nature* 373:623–6

Wagle N, Emry C, Berger MF *et al.* (2011) Dissecting therapeutic resistance to RAF inhibition in melanoma by tumor genomic profiling. *J Clin Oncol*; e-pub ahead of print 7 March 2011

Wagner KW, Punnoose EA, Januario T *et al.* (2007) Death-receptor O-glycosylation controls tumor-cell sensitivity to the proapoptotic ligand Apo2L/TRAIL. *Nat Med* 13:1070–7

Ye X, Li Y, Stawicki S *et al.* (2010) Anti-Axl monoclonal antibody attenuates xenograft tumor growth and enhances the effect of multiple anticancer therapies. *Oncogene* 29:5254–64

Zendman AJ, Ruiter DJ, Van Muijen GN (2003) Cancer/testis-associated genes: identification, expression profile, and putative function. *J Cell Physiol* 194:272–88

Zhu S, Wurdak H, Wang Y *et al.* (2009) A genomic screen identifies TYRO3 as a MITF regulator in melanoma. *Proc Natl Acad Sci USA* 106: 17025–30